JOURNAL OF MATERIALS SCIENCE 7 (1972) 159–167

The Matrix Fatigue Behaviour of Fibre Composites Subjected to Repeated Tensile Loads

ARI VARSCHAVSKY
Instituto de Investigaciones y Ensayos de Materiales, Facultad de Ciencias Físicas y Matemáticas, Universidad de Chile, Santiago, South America

In a fibre/metal matrix composite the mechanical properties of the matrix itself are changed by the presence of the reinforcing fibres. This changed behaviour of the metal is referred to as *in situ* behaviour, and a phenomenological model is developed to evaluate the *in situ* plastic stress-strain properties of a metallic matrix containing fibres, from a study of the properties of the composite. The model is based upon the idealised behaviour of the two components of the system. The application of the model to B/Al alloy composites shows that the plastic stress-strain behaviour of the matrix containing fibres varies strongly with the fibre volume content, and also that the matrix *in situ* cyclic stress-strain behaviour can be approximately described by a power law of the type: $\phi' = \phi_0([\Delta\epsilon'_p]/2)^n$, where the strength coefficient and the exponent increase with the fibre volume fraction. It also predicts that in the steady state fatigue behaviour of the composites, the fraction of load amplitude carried by the fibres decreases with increasing applied stress amplitude, and is also dependent on the fibre volume fraction. The effect of the applied stress on the damping capacity is established through expressions derived from the basic ideas involved in the model.

1. Introduction

In composite materials consisting of fibres in a metal matrix, the onset of plastic flow in the metal matrix leads to deviation from a linear stress-strain relationship [1, 2]. For instance, it has been shown [2] that, under a cyclic stress, many composites develop, after the first few cycles, a stress-strain curve forming a closed hysteresis loop (referred to hereafter as the stabilised loop) reproducible for a great number of stress cycles. The presence of the reinforcing fibres stiffen the composite by carrying the load but there is an additional effect due to the fact that the properties of the matrix itself are changed by the presence of the fibres. The work presented is mainly concerned with determining the extent of this change in matrix properties. The data are interpreted on the basis of a model developed in section 2. This model is an extension of the model of Baker and Cratchley [2] to steady state conditions in fatigue.

2. The Cyclic Stress-Strain Model

The mechanical properties of the metal matrix itself are changed by the presence of the reinforcing fibres; this changed behaviour will be referred to as *in situ* behaviour in contrast to the behaviour of the same metal without reinforcement. A model is developed which permits the determination of the *in situ* behaviour from cyclic stress-strain and normal (monotonic) stress-strain data of the composite. The model is an extension to a model given by Baker and Cratchley [2]. Therefore, the preliminary part of the model is given schematically using fig. 1, and reference must be made to [2] for full details. The model supposes that (1) the Bauschinger effect may be neglected; (2) a stabilised hysteresis loop exists for the matrix under cyclic stress; (3) this hysteresis loop shows well-defined elastic and plastic regions and zero slope in the plastic region (fig. 1a).

Fig. 1a shows stabilised hysteresis loops for the unreinforced metal subjected to two different

values of the cyclic stress in the range $\pm \phi_1$, and $\pm \phi_2$ respectively. The cyclic stress-strain curve (dotted line) is the locus of the vertices of the rectangles in fig. 1b, where the elastic strain was subtracted.*

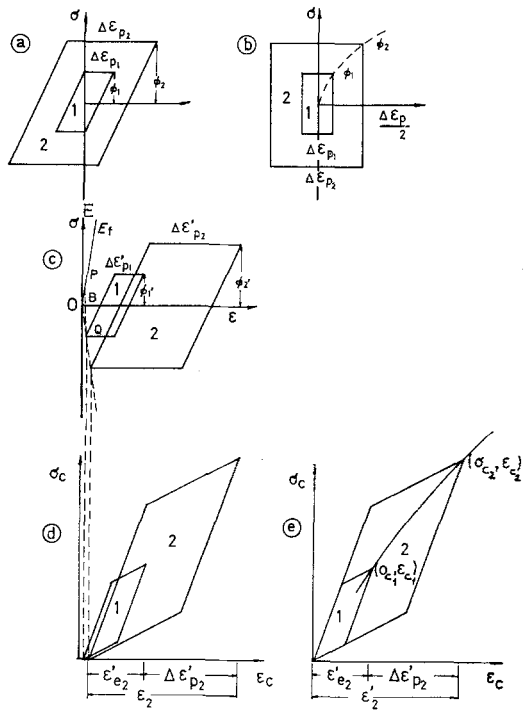

Figure 1 Schematic development of the stress-strain behaviour of the composite and each component under saturation conditions. For explanation see the text.

Fig. 1c represents separately the behaviour of the fibres and matrix of the composite material subject to repeated tensile stress in the range 0 to σ_c while the matrix is subject to a cyclic stress, in the range $\pm \phi'_1$, $\pm \phi'_2$ respectively. OE is the stress-strain curve for the fibre which is always in the elastic region and shows no hysteresis. The loops represent the matrix behaviour where the loop position can be determined by considering that at the completion of a cycle the tension in the fibre (BP) must be equal to the compressive stress in the matrix (BQ). In this case the hysteresis loops of the matrix represent the *in situ* behaviour and therefore the parameters are not necessarily equal to those of fig. 1a, and are marked with primes.

Using this diagram, the cyclic behaviour of the composite as a whole can be constructed (fig. 1d). Since only the stabilised cyclic behaviour is considered the original origin of strain is not important and the curves are redrawn taking the zero stress condition of the cyclic behaviour as the zero of strain (fig. 1e). The curves have the form of parallelograms with slopes E_1, a compromise between the elastic behaviour of fibre and matrix and E_2, the result of elastic deformation in the fibre and plastic deformation of the matrix. Note that while the fibres are always in tension, from zero to some upper value, the matrix is alternately in tension (upper half of parallelogram) and compression (lower half). The locus of the vertices (σ_c, ϵ_c) of the loops gives cyclic stress-strain data for the composite.

By inspection of fig 1e the following relations may be written:

$$\sigma_c = \frac{2\phi' E_1}{E_m'} + E_2 \, \Delta\epsilon_p' \qquad (1)$$

$$\epsilon_c = \frac{2\phi'}{E_m'} + \Delta\epsilon_p' \qquad (2)$$

σ_c is the cyclic stress amplitude for the composite, while the matrix is subject to a cyclic stress range of $\pm \phi'$ (hence $2\phi'$ in equations 1 and 2); ϵ_c is the cyclic strain amplitude of the composite and $\Delta\epsilon_p'$ the plastic strain range. E_m' is the *in situ* elastic modulus of the matrix and may be anticipated to lie between E_m and E_1, where E_m is the elastic modulus of the unreinforced matrix. The combination of equations 1 and 2 gives

$$\sigma_c = \frac{(E_1 - E_2)\, 2\phi'}{E_m'} + E_2 \, \epsilon_c \qquad (3)$$

or

$$\phi' = \frac{(\sigma_c - E_2 \, \epsilon_c) \, E_m'}{2 \, (E_1 - E_2)} \qquad (4)$$

In order to use these relations a value of E_m' is needed. In subsequent paragraphs the problem of its determination is considered.

The monotonic (i.e. non-cyclic) stress-strain curve has, in general, two well-defined regions: stage I where both fibres and matrix behave elastically and stage II where the fibres behave elastically and the matrix plastically. However, the monotonic modulus in stage I, E_c, is not generally equal to E_1. In other words, although in both cases both components of the composite are deforming elastically, there is a difference

*A cyclic stress-strain curve is defined as $\phi' = f([\Delta\epsilon'_p]/2)$. [3]

in the modulus under cyclic and monotonic loading. Therefore, under fatigue test conditions, it is possible that both the fibre and matrix moduli are different from the unreinforced situation and different too from the values in the composite material under monotonic conditions. However, it has been shown [4, 5] that the fibre modulus under monotonic conditions is the same as the modulus of the free fibre. Thus, using a modified rule of mixtures [4, 6),

$$E_c = E_f V_f + (1 - V_f) E_m'' \qquad (5)$$

it is possible to calculate E_m'', the monotonic modulus of the matrix *in situ*, where E_f and V_f are the free fibre modulus and volume fraction of fibre respectively.

The difference between E_c and E_1 may be due to changes in E_f under cyclic conditions or because $E_m'' \neq E_m'$, or both. It is reasonable to suppose, failing further experimental data or a decisive model, that both moduli change and that the situation is bounded by the possible conditions $E_m'' = E_m'$ or E_f unchanged. However, in the present case, the difference between E_c and E_1 was small and the separation between these bounds gives values of ϕ' which differ only by the order of the experimental error. Therefore, because E_c could be determined with greater precision than E_1, the calculations of E_m' were all performed using equation 5 and supposing $E_m'' = E_m'$.

3. Experimental Procedure

Two 6061-T6 aluminium/boron composite plates with 25 and 40 % by volume of boron filaments in continuous and unidirectional reinforcement, were used in order to apply the model. In the composite fabrication process, an assembly of aluminium sheets 0.126 mm thick and boron filaments of 0.1 mm nominal diameter were disposed in alternative layers and hot pressed at 975°F (524°C) for 30 min to promote diffusion bonding. The composites were next heat treated at 950°F (510°C) for 10 min, cold water quenched and aged at 350°F (177°C) for 6 h.

The test specimens were straight-sided with tabs bonded on to the faces in the gripping areas, in order to minimise stress concentration and damage. The bonded doublers that have been utilised on the specimens were made from a 6061 aluminium bar having approximately the same thickness as the composite tested. They were bonded to the specimen sides with Hysol-Epoxi. Specimens reinforced with 40 % boron filaments were 38 mm long, 6.1 mm wide, with a thickness of 0.81 mm. Each specimen contained about 365 filaments disposed in five layers. Specimens reinforced with 25 % boron filaments were 47 mm long, 1.06 mm wide and 0.60 mm thick. The specimens contained approximately 170 filaments distributed in four layers. All specimens were prepared in a Servomet spark cutting machine.

Tension/tension tests on the composite specimens were carried out in an Instron machine, at a crosshead speed of 0.02 cm/min.

4. Experimental Results

4.1. The Cyclic Stress-Strain Curve

Figs. 2 and 3 show a series of stabilised hysteresis loops for 40 and 25 % of volume fibre content respectively. In this figure the dashed lines represent the tangent at the origin and at the tip of each stable loop. The slopes of the dashed lines appearing in figs. 2 and 3 are the primary and secondary moduli for the corresponding loop. As can be observed, the variations in both quantities from one specimen to another are very small, therefore for each composite E_1 and E_2 were obtained by averaging the values measured from stabilised hysteresis loops for different applied stress amplitudes. The error introduced by using average values will be estimated later. E_1 and E_2 values are shown in table I.

TABLE I

	Material	
Modulus	40 % B/Al	25 % B/Al
	6061-T6	6061-T6
E_1 (kg/mm²)	27.5×10^3	18.0×10^3
E_2 (kg/mm²)	17.0×10^3	10.6×10^3

The cyclic tension/tension stress-strain curves for the 6061-T6 aluminium alloys reinforced with boron filaments are shown in fig. 4 for 25 and 40 % reinforcement. These curves were obtained from figs. 2 and 3 by plotting the applied stress against the stabilised strain. The monotonic stress-strain curves for both composites are also plotted in this figure where it can be observed that the monotonic curves are lower than the cyclic tension/tension curves, due to the change in origin of strain in the latter case, and also to work hardening of the matrix

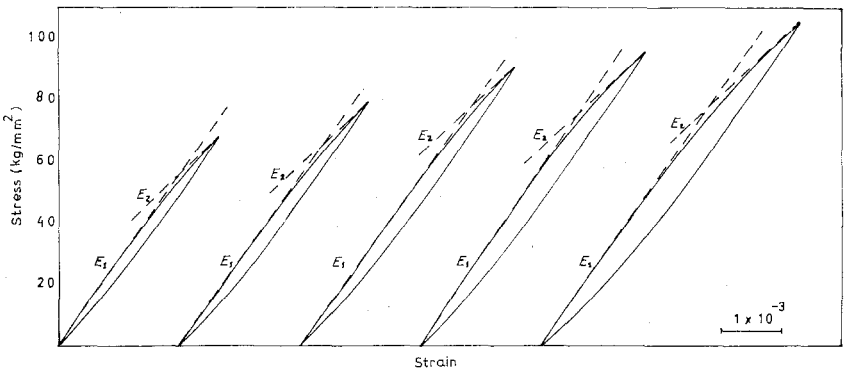

Figure 2 Stabilised hysteresis loops for a 6061-T6 aluminium alloy reinforced with 40% of boron filaments after 20 cycles.

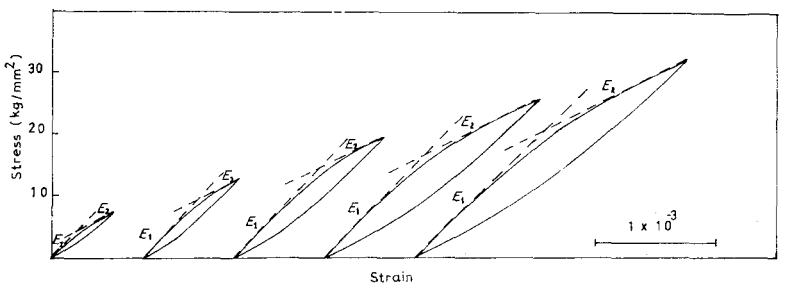

Figure 3 Stabilised hysteresis loops for a 6061-T6 aluminium alloy reinforced with 25% of boron filaments after 20 cycles.

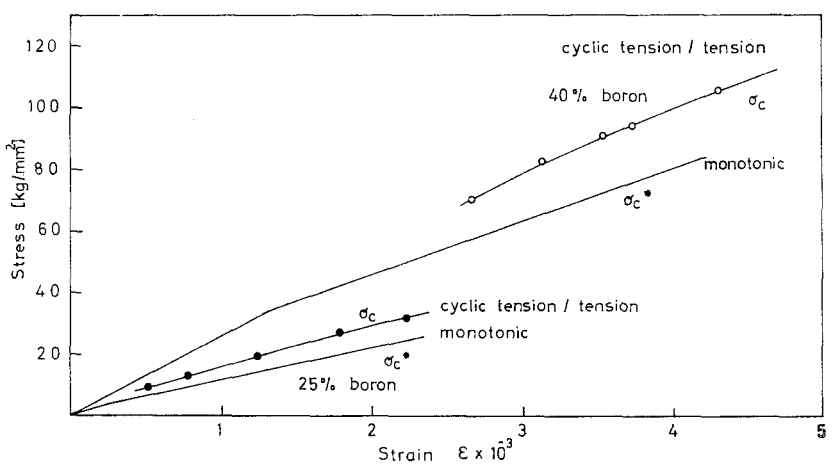

Figure 4 Cyclic tension/tension and monotonic stress-strain curves for B 6061-T6 composites.

as will be shown later from microhardness measurements.

The *in situ* matrix modulus E_m' was next computed for insertion in equation 4. This was accomplished by using equation 5 in which respective values of E_c must be determined. From the monotonic stress-strain curves $E_c = 17 \times 10^3$ kg/mm² for 25 % of reinforcement and $E_c = 26 \times 10^3$ kg/mm² for 40 %. By using $E_f = 38.5 \times 10^3$ kg/mm² [5, 7], one obtains from equation 5:

$$E_m' = 9.9 \times 10^3 \text{ (kg/mm}^2\text{)}$$

for 25 % of reinforcement, and

$$E_m' = 17.4 \times 10^3 \text{ (kg/mm}^2\text{)}$$

for 40 % of reinforcement.

Introducing the corresponding values of E_1, E_2 and E_m' for each composite in equations 2 and 4, we find that:

$$\phi' = 0.70\,(\sigma_c - 10.6 \times 10^3\,\epsilon_c) \text{ (kg/mm}^2\text{)} \quad (6)$$

$$\epsilon_c = 0.20 \times 10^{-3}\,\phi' + \Delta\epsilon_p' \quad (7)$$

for 25 % of boron fibre content, and

$$\phi' = 0.83\,(\sigma_c - 17 \times 10^3\,\epsilon_c) \text{ (kg/mm}^2\text{)} \quad (8)$$

$$\epsilon_c = 0.12 \times 10^{-3}\,\phi' + \Delta\epsilon_p' \quad (9)$$

for 40 % of boron fibre content.

From each set of equations a function $\phi' = f(\Delta\epsilon_p'/2)$ can be plotted for both composites, using corresponding values of σ_c and ϵ_c from the data of fig. 4; the results obtained are shown in fig. 5. It can be seen from fig. 5 that at the same plastic strain amplitude the cyclic stress in the matrix (yield stress) ϕ' reaches much higher values when the percentage of boron filaments in the composite is higher.

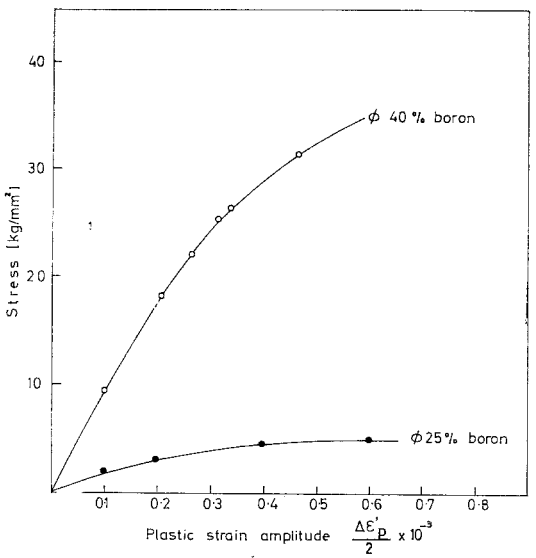

Figure 5 In situ cyclic stress-strain curves for the matrix in Al 6061-T6 boron reinforced composites.

Fig. 5 is replotted on a log-log scale in fig. 6. It is observed that the *in situ* cyclic stress-strain curves can be drawn to a first approximation as straight lines in these figures; thus the function $\phi' = f(\Delta\epsilon_p'/2)$ can be expressed by a power law:

$$\phi' = \phi_0\,(\Delta\epsilon_p'/2)^n .$$

The strength coefficient ϕ_0 and the strain hardening exponent "n" were determined from least square analysis of the data points. The values of "ϕ_0" and "n" are listed in table II.

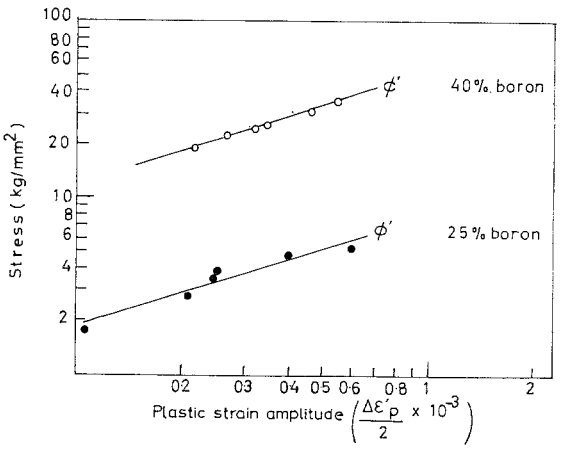

Figure 6 Log-log plot of curves appearing in fig. 5.

TABLE II

Material	ϕ_0 (kg/mm²)	n
Al 6061-T6/40 % B	5	0.7
Al 6061-T6/25 % B	340	0.6

It can be noticed that the hardening exponent, and the strength coefficient, increase with increasing reinforcement. The comparison between the curves cannot be regarded as absolute since the hardening state of the matrix before the fatigue tests is different for different fibre volume fractions. This occurs because of the development of residual stresses in the composite due to cooling from the fabrication temperature.

Calculation of the residual stresses resulting from the differences between the coefficients of thermal expansion of the matrix and the filaments shows that stresses higher than those needed for plastic flow are developed during the composite cooling. In fact, for filament spacing greater than filament diameter, the elastic radial stress σ_{rr} is given by [8]:

$$\sigma_{rr} = -\alpha\Delta T\left(\frac{3a^2}{2r^2} - \frac{1}{2}\right)E_m \quad (10)$$

where $\alpha = \alpha_m - \alpha_f$, "$a$" is the filament radius and ΔT the cooling temperature range. E_m is the matrix modulus (7.03×10^3 kg/mm²).

The distance from the centre of a filament to a point in the matrix ("r"), for which the elastic radial stress is equal to the yield stress of the

matrix (28 kg/mm²), was computed for the boron reinforced composites. With $\Delta T = 900°F$ (482°C), $a = 51 \times 10^{-3}$ mm, $\alpha_m = 14.1 \times 10^{-6}$ mm/mm°F (= 7.83 mm/mm°C) and $\alpha_f = 4.6 \times 10^{-6}$ mm/mm°F (= 2.55 mm/mm°C) "r" $= 62 \times 10^{-3}$ mm. This corresponds to a distance of 11.8×10^{-3} mm from the fibre surface. That is, for a distance less than 11.8×10^{-3} the radial stress would exceed the room temperature yield stress of the matrix.

The fraction of matrix volume, "C", for which the radial stress exceeds the matrix yield stress at room temperature is next computed by using the following relation:

$$C = V_f \frac{(r^2/a^2 - 1)}{1 - V_f} \tag{11}$$

Substituting in this expression the value of "a" and "r" already computed, "C" becomes 0.16 and 0.32 for 25 and 40 % of boron content, respectively.

The above computations indicate that for 40 % of boron filament content the average work hardening in the matrix must be higher than for 25 % of boron filament content, in the fabricated composite prior to the fatigue test. Hardness measurements confirm this argument; for instance, the average Vickers microhardness taken in a virgin specimen matrix was 91 and 70 for 40 and 25 % by volume of fibre, respectively.

4.2. The Fraction of Load carried by the Fibres

The model here developed can be used to compute the fraction "B" of tensile load amplitude on the composite which is carried by the fibres at the tip of a stabilised hysteresis loop. This fraction is given by:

$$B = 1 - \frac{\phi'}{\sigma_c}(1 - V_f) \tag{12}$$

Substitution of equation 4 in equation 12 gives:

$$B = 1 - \frac{E_m'(\sigma_c - E_2 \epsilon_c)(1 - V_f)}{2(E_1 - E_2)\sigma_c} \tag{13}$$

Introducing respective values of E_m', E_1, E_2 and V_f in equation 13, "B" can be evaluated for each set of values σ_c and ϵ_c obtained from fig. 4. A curve showing "B" as a function of the applied stress σ_c on the composite is shown in fig. 7, for both fibre volume fractions. It is observed in this figure that "B" decreases more abruptly for the composite with 25 % of fibre reinforcement and also that the values of "B" are somewhat higher for this fibre content.

The first of these two effects indicates that the percentage of hardening undergone by the matrix reinforced with 25 % of boron filaments is greater when the load amplitude is increased. In fact, due to the fabrication process, the matrix was in a lower hardening state "H" prior to the fatigue test for 25 % of boron content, as explained in section 4.1. The subsequent rate of fatigue hardening, $dH/d\sigma_c$, is expected to be higher for this fibre volume fraction; this implies a higher rate of stiffening of the matrix. Since one of the important factors influencing the transfer of load to the fibres is the ratio between the stiffness of the fibres and the matrix which must be the highest possible [2], a higher value of the rate of stiffening of the matrix necessarily leads to a more pronounced decrease of "B" with σ_c.

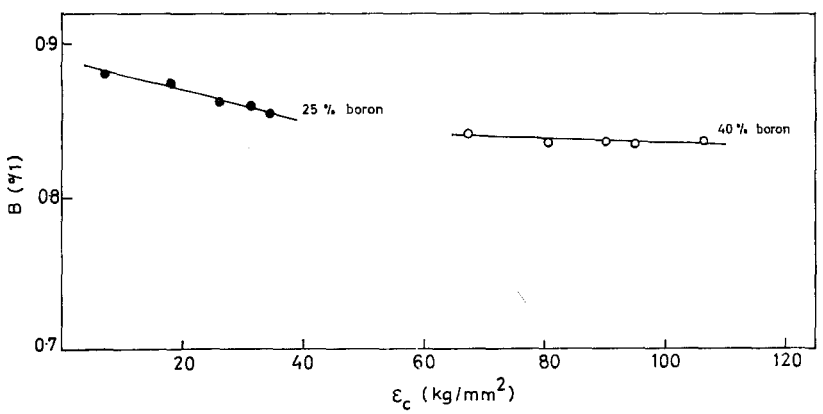

Figure 7 Fraction of load B carried by the fibres as a function of the applied stress on the composite.

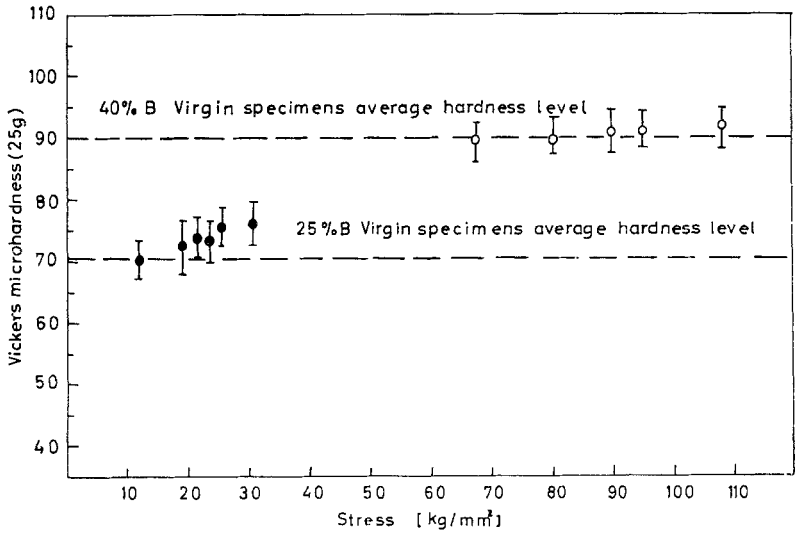

Figure 8 Vickers microhardness versus applied stress amplitude for B 6061-T6 Al composites at the steady state behaviour.

To show it is true that the rate of stabilised hardening $dH/d\sigma_c$ is higher for the matrix reinforced with 25 % of boron filaments, the Vickers microhardness of the fatigued specimens was measured; the results are shown in fig. 8.

Despite the higher values of "B" which are expected for the 40 % boron composite, simply because of the greater volume fraction of fibre, the values are very similar for both composites (fig. 7). However in the 40 % boron composite, even before the fatigue tests, the aluminium-aluminium diffusion bonds have been found disrupted near the fibre surfaces due to imperfections in the fabrication process. After the fatigue tests complete delamination of the aluminium-aluminium diffusion bonds was observed in the same regions, as illustrated in a fractured specimen in fig. 9. This had reduced the effective fibre-matrix interface leading to a loss of efficiency in the transfer of load to the fibres. This can explain the similar values obtained for both 25 and 40 % boron reinforcement.

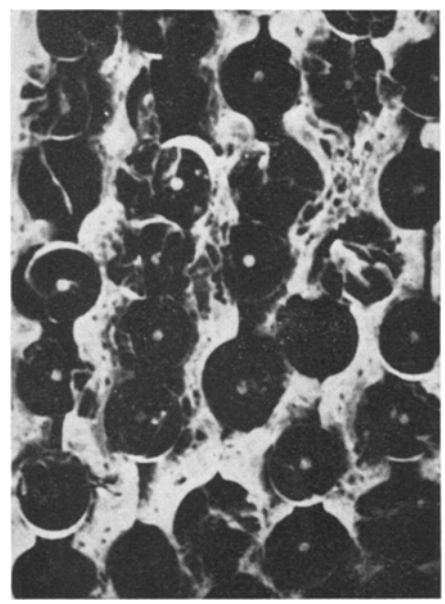

Figure 9 Scanning electron micrograph of a fatigued specimen with 40% of boron filaments. It can be observed delamination of the aluminium-aluminium bonds. ($\sigma_c = 95$ kg/mm^2; $N = 25$ cycles).

4.3. Damping Behaviour

The specific damping capacity is conventionally defined [2] as

$$P = \frac{\text{energy absorbed during one loading cycle}}{\text{maximum stored energy}}$$

where the maximum stored energy is approximately $\frac{1}{2}\,\sigma_c\epsilon_c$. The energy absorbed may be estimated from the area of the loop or, in the approximation of the model, calculated from the geometry of the parallelogram (fig. 10), giving:

$$\text{Absorbed energy} = (\sigma_c - E_2\,\epsilon_c)\,\Delta\epsilon_p' \quad (14)$$

Where the meaning of each symbol has been previously defined. Substituting for $\Delta\epsilon_p'$ from equation 2 and using equation 4 to eliminate ϕ', we have:
Absorbed energy =

$$\frac{(\sigma_c - E_2\,\epsilon_c)\,(E_1\,\epsilon_c - \sigma_c)}{E_1 - E_2} \tag{15}$$

Then the stabilised specific damping capacity is given by:

$$P = \frac{2(\sigma_c - E_2\,\epsilon_c)\,(E_1\,\epsilon_c - \sigma_c)}{\sigma_c\,\epsilon_c\,(E_1 - E_2)} \tag{16}$$

Introducing the "secant" modulus of the composite, $E_s = \sigma_c/\epsilon_c$, equation 16 becomes:

$$P = \frac{2\,(E_s - E_2)\,(E_1 - E_s)}{E_s\,(E_1 - E_2)} \tag{17}$$

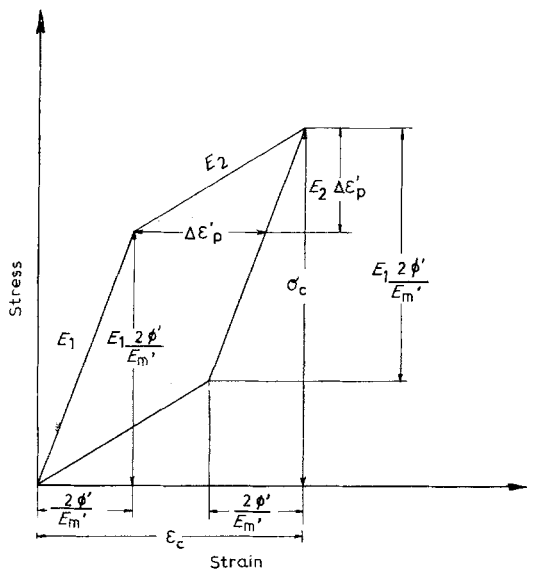

Figure 10 Schematic representation of composite hysteresis behaviour at a particular stress level.

For convenience equation 17 was used to calculate P in these experiments. In this case for constant E_1, E_2 the P has a maximum value for

$$E_s = (E_1\,E_2)^{1/2} \tag{18}$$

A plot of the specific damping capacity versus the secant modulus in Al 6061-T6 boron reinforced composites is shown in fig. 11. This curve was obtained by using equation 17. As can be expected, higher values of "P" are obtained for 25 % of boron reinforcement. This kind of damping can be attributed to internal friction depending upon stress amplitude, which is invariably associated with unpinning and movement of dislocations [9] leading to plastic deformation in the matrix. Therefore this observed behaviour may be explained by the fact that the matrix reinforced with 25 % of boron fibres is able to undergo a higher degree of plastic deformation than that with 40 % of boron reinforcement.

As E_s decreases with increasing values of σ_c, the stabilised damping capacity increases with the applied stress in the range of stresses used in performing the fatigue tests. Although the maximum of the curve was not reached in the present experiments since this maximum occurs near the fracture stress of the tested composites, it has been confirmed for an aluminium/silica and an aluminium/stainless steel composite [10]. The reason for the maximum with stress has been explained [10] by attributing a more rapid build-up of elastic energy compared to the loss of energy due to plastic deformation.

5. Accuracy of the Method

The hysteresis loops of the B/Al composites, for which the *in situ* cyclic stress-strain model of the matrix has been used, showed that the values of E_1 and E_2 remain almost constant with the applied stress amplitude. The error introduced by using the average values of E_1 and E_2 in equation 4 have to be estimated. By differentiating this equation and by dividing it by ϕ' it is found that:

$$\frac{\Delta\phi'}{\phi'} = \frac{(\sigma_c - \epsilon_c\,E_1)\;\Delta E_2}{(\sigma_c - \epsilon_c\,E_2)\;(E_1 - E_2)} \tag{19}$$

The values of E_1 had a negligible dispersion and the values of E_2 had a dispersion of 5 and 10 % for 25 and 40 % reinforcement respectively. The corresponding error in ϕ' was 5 and 1 %.

In other composites for which E_1 and E_2 may not be constant, the expressions here developed to compute ϕ' do not suffer any change; in this case the values of ϕ' in equation 4 must be computed for the respective values of E_1, E_2, σ_c and ϵ in each hysteresis loop.

Finally, the values of ϕ' are somewhat underestimated when it is assumed that there is zero slope in the plastic region of the matrix stabilised hysteresis loops. The damping capacity values are also higher than the real ones because a parallelogram was considered when computing the areas of the hysteresis loops.

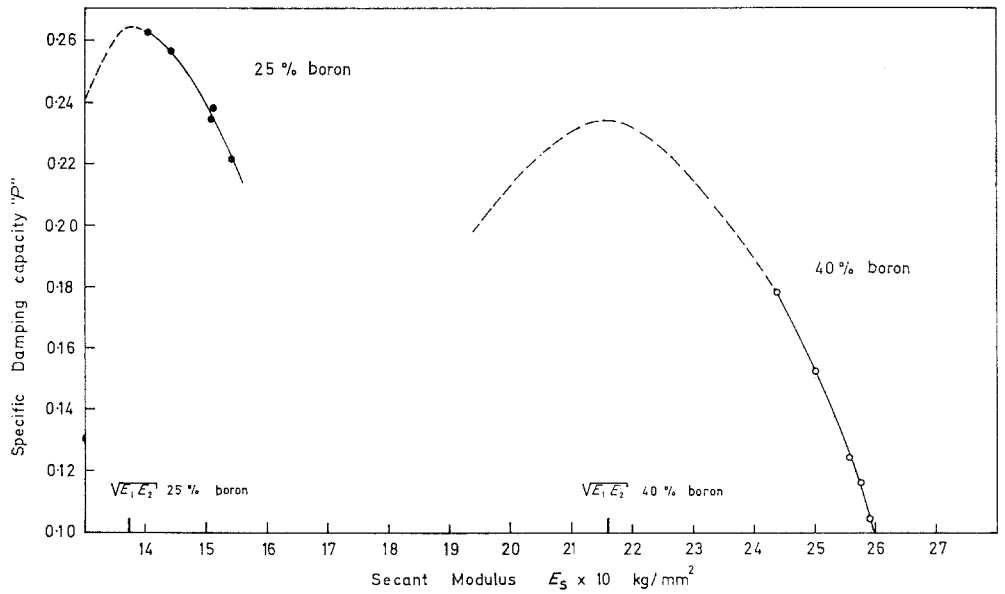

Figure 11 Specific damping capacity versus secant modulus for Al 6061-boron reinforced composites.

This model has the advantage, as has been pointed out, of considering the presence of synergistic effects in the composite, since the expressions here developed make use of the experimental values of the primary and secondary moduli E_1 and E_2.

Acknowledgements

The author is indebted to Dr John Eades for his continued interest, advice and fruitful discussions. He would also like to thank Dr Russel C. Jones for the Scanning Electron Microscope facilities made available to him at the Massachusetts Institute of Technology; Miss María I. Pérez for help with the experiments and María R. Marrapodi for her generous help. Acknowledgements for financial support are due to Instituto de Investigaciones y Ensayes de Materiales, Universidad de Chile.

References

1. D. L. MCDANIELS, R. W. JECH, and J. W. WEETON, *Trans. Met. Soc. AIME* **233** (1965) 636.
2. A. A. BAKER and D. CRATCHLEY, *Appl. Mat. Res.* **5** (1966) 92.
3. C. A. FELTNER and C. LAIRD, *Acta Metallurgica.* **15** (1967) 1921.
4. D. L. MCDANIELS and J. W. WEETON, *Met. Prog.* **78** (1960) 118.
5. W. F. STUHRKE, in Metal Matrix Composites Symposium. Seventieth Annual Meeting, *Am. Soc. Test. Mat.* Boston, Mass. (1967) 108.
6. J. R. HANCOCK and J. C. GROSSKREUTZ, *ibid.* (1967) 134.
7. E. BRENNAN, *Met. Trans.* **1** (1970) 309.
8. R. L. MEHAN, in Metal Matrix Composites Symposium. Seventieth Annual Meeting, *Am. Soc. Test. Mat.* Boston, Mass. (1967) 29.
9. A. GRANATO and K. LUCKE, *J. Appl. Phys.* **27** (1965) 583.
10. A. A. BAKER, *J. Mater. Sci.* **3** (1968) 412.

Received 28 July and accepted 3 September 1971.